CORROSION SCIENCE AND TECHNOLOGY, Vol.9, No.2(2010), pp.92~97

Evaluation of Metals (Al, Fe, Zn) in Alternative Fuels by Electrochemical Impedance Spectroscopy in Two Electrode Cell

Yon-Kyun Song[1], Geunwoong Lim[2], and Heesan Kim[2,†]

[1]*POSCO Technical Research Laboratories Gumho-dong, Gwangyang, Jeonnam 545-090, KOREA*
[2]*Hongik University 300, Sinanri, Yeongigun, Chochiwoneup, Chungnam, 339-701, KOREA*
(Received August 3, 2009; No Revision; Accepted April 8, 2010)

Many kinds of alternative fuels such as biodiesel, ethanol, methanol, and natural gas have been developed in order to overcome the limited deposits in fossil fuels. In some cases, the alternative fuels have been reported to cause degrade materials. The corrosion rates of metals were measured by immersion test, a kind of time consuming test because low conductivity of these fuels was not allowed to employ electrochemical tests. With twin two-electrode cell newly designed for the study, however, electrochemical impedance spectroscopy (EIS) test was successfully applied to evaluation of the corrosion resistance (R_p) of zinc, iron, aluminum, and its alloys in an oxidized biodiesel and gasoline/ethanol solutions and the corrosion resistance from EIS was compared with the corrosion rate from immersion test. In biodiesel, R_p increased in the order of zinc, iron, and aluminum, which agreed with the corrosion resistance measured from immersion test. In addition, on aluminum showing the best corrosion resistance (R_p), the effect of magnesium as an alloying element was evaluated in gasoline/ethanol solutions as well as the oxidized biodiesel. R_p increased with addition of magnesium in gasoline/ethanol solutions containing chloride and the oxidized biodiesel. In the mean while, in gasoline/ethanol solutions containing formic acid, Al-Mg alloy added 1% magnesium had the highest R_p and the further addition of magnesium decreased R_p. It can be explained with the fact that the addition of more than 1% magnesium increases the passive current density of Al-Mg alloys.

Keywords *: biodiesel, ethanol, polarization resistance, twin two-electrode cell*

1. Introduction

The limited deposits in fossil fuels cause many kinds of alternative fuels such as biodiesel, ethanol, methanol, natural gas to be developed. The wide usage of these alternative fuels as an automotive fuel has required automotive makers to develop materials compatible to these fuels. Some alternatives have been reported to corrode and wear materials and to degrade fluidity of the alternatives.[1),2)] Biodiesel and ethanol among these alternatives were used in this study because ethanol is relatively corrosive, and the auto-oxidation of biodiesel induces to induce corrosive environments.[3)] In addition, more reliable metals and polymers are required to be selected because the degradation of materials applied to an automotive fuel system can decrease the fluidity of the fuels.[1),2),4)] As a method for evaluating reliability of materials, immersion test has been mainly used despite of a time consuming test because the electrochemical method has not been available due to low conductivities of the alternatives (ns/cm ~ μs/cm).[5)-10)]

In the study, to overcome a shortcoming of electrochemical methods, a twin two-electrode cell[11)] where the distance between two electrodes is controllable at the rage 100 μm to 1 cm was designed to measure polarization resistance (R_p) using electrochemical impedance spectroscopy (EIS). In addition, the effects of magnesium on the corrosion rate of Al-Mg alloys were evaluated by measurement of R_p in the oxidized biodiesel and gasoline/ethanol solutions containing NaCl or formic acid.

2. Experiment

2.1 Immersion test

Immersion test was carried out to evaluate corrosion behaviors of zinc, iron, and aluminum in an oxidized biodiesel and to compare the corrosion behaviors from the immersion with corrosion behavior from EIS. For the test, biodiesel was oxidized as followed: the biodiesel where 2% 2-etylhexyl nitrate (EHN, 97%) as an oxidant was add-

† Corresponding author: heesankim@yahoo.co.kr

ed was heat up to 160 ℃ for 48 hours, and air was flown through the biodiesel with the rate of 500 cc/min during oxidation. In some case, 4% formic acid was added to further accelerate corrosion rate after oxidation. The properties of biodiesel solutions used in the test are summarized in Table 1. Prior to immersion, the surface of specimen was grinded up to 1200 grit SiC paper, washed with distilled water, and degreased with acetone, and ethyl alcohol, sequently. After the specimens were immersed in the test solutions for 3, 7, 15, and 28 days, the corrosion products on metal surface were removed according to ASTM G1-03 as follows: zinc was cleaned by immersion for 4 min in 1.87 M NH_4Cl at 70 °C, iron was cleaned by 3 min immersion in 0.025 M $C_6H_{12}N_4$ + 5.43 M HCl at 20 °C, and aluminum was cleaned by 3 min in 60% HNO_3 at 20 °C. Finally, the weigh was measured.

2.2 Potentiodynamic test

Potentiodynamic test was carried out to examine the effects of magnesium on corrosion resistance of Al-Mg alloys (pure Al, Al-1%Mg, Al-10%Mg, and Al-20%Mg) in the oxidized biodiesel and gasoline/ethanol solutions. As gasoline/ethanol solutions, the following solutions were used: E50+5% water +330 ppm NaCl, E50+5% water +100 ppm formic acid, E85+5% water +330 ppm NaCl, and E85+5% water +100 ppm formic acid. Typical 1L-electrochemical cell was used. The specimen was treated as mentioned in '2.1 immersion test' and electrically connected using flat specimen holder. A saturated calomel electrode (SCE) and a platinum electrode were used as a reference electrode and a counter electrode, respectively. Potential was anodically polarized from corrosion potential to -0.3 V with a scan rate of 60 mV/min after corrosion potential (E_{corr}) was stabilized.

2.3 Electrochemical impedance spectroscopy (EIS) test

EIS test was carried out in order to measure the polarization resistance of aluminum and its alloys, iron, and zinc in the oxidized biodiesel and the gasoline/ethanol solutions with high resistivity. Twin two-electrode cells were designed for measurement of polarization resistance (R_p) using EIS in solutions with high resistivity as shown in Fig. 1 and Fig. 2. Especially, in the cell (Fig. 1), the distance between two electrodes is controllable at the rage 100 μm to 1 cm to measure R_p in a solution having extremely low conductivity such as biodiesel solution whose resistivity is 5 nS/cm. In addition, in order to minimize unwanted crevice corrosion between specimen and masking materials, the sides of the specimens were painted with an coating material (Amercoat, AMERON Co.), dried at 50 °C for 24 hour, and then cold-mounted with the cold resin. The surface of the specimen was grinded up to 1200 grit SiC paper. The specimen was washed with distilled water and degreased with acetone and ethyl alcohol, sequently. EIS test was performed after 30- min immersion for stabilization of the corrosion potential (E_{corr}). EIS measurement was performed at the corrosion potential with voltage perturbation amplitude of 10 mV in the frequency range from 0.005 to 10^6 Hz. In case of biodiesel,

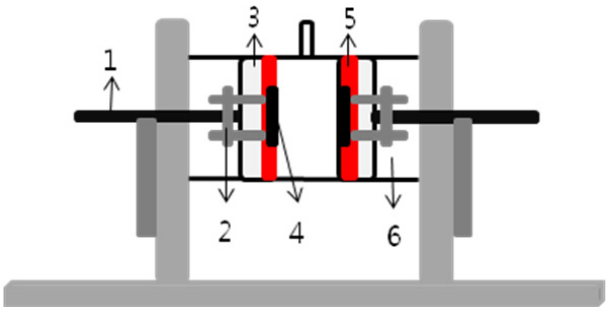

Fig. 1. Twin two-electrode cell used for biodiesel, consisting of (1) micro meter, (2) electrical connector, (3) teflon specimen holder (4) specimen, (5) teflon O-ring, and (6) glass tube.

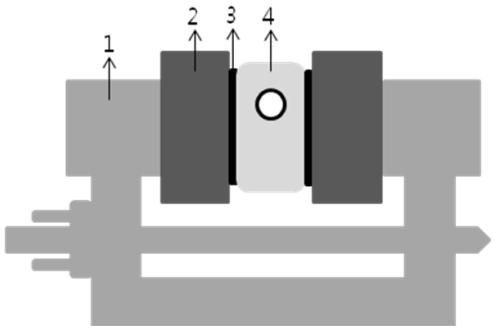

Fig. 2. Twin two-electrode cell used for ethanol mixed solutions, consisting of (1) clamp for cell assembly, (2) specimen, (3) O-ring, and (4) teflon tube.

Table 1. Biodiesel solutions used for immersion tests and their properties

Composition	Oxidation conditions (temperature (℃)/holding time (hrs))	Acidity (KS M ISO 6618) (mg KOH/g)	Conductivity (μS/cm)
Bio-D+2%EHN	165/48	30.2	0.005
Bio-D+2%EHN 4%HCOOH	165/48	82.5	0.197

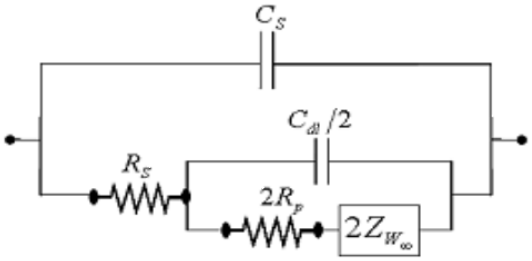

Fig. 3. Electrical equivalent circuit. (C_s: solution capacitance, C_{dl}: double-layer capacitance, R_s: solution resistance, R_p: polarization resistance, Z_w: Warburg impedance)

the distance between two electrodes was 50 μm which the open circuit current is stable without oscillation. In case of gasoline/ethanol solution, the electrochemical cell (Fig. 2) was chosen, where the distance between electrodes and area of the surface were 8 mm and 2.54 cm^2. The polarization resistance (R_p) was analyzed using equivalent circuit as shown in Fig. 3 and data fitting program (Autolab FRA).

3. Result and discussion

3.1 Corrosion rates of Zn, Fe, and Al in oxidized biodiesel

Fig. 4 shows the mass gain of zinc, iron, and aluminum with immersion in the oxidized biodiesel. The addition of formic acid to the oxidized biodiesel increased the corrosion rates of the metals, which was explained with the following reaction:

$$aM + bHCOOH \leftrightarrow M_a(COOH)_b + \tfrac{b}{2}H_2 \qquad (1)$$

The above reaction was confirmed by the observation of the diffraction peaks of acetate on corerosion product by XRD. The corrosion rate of zinc and aluminum were the highest and the lowest, respectively. In addition, the corrosion kinetics correxpond to a parabolic bahavior, which probably is due to the formation of corrosion product layer.

Fig. 5(a) shows the nyquist plot of zinc in the oxidized biodiesel representing one semi-circle in a higher frequency region and one loop in a lower frequency region. The semi-circle in the higher region was due to the resistance of the biodiesel. It was proved by the comparison between resistivity calculated from the semi-circle and resistivity measured from conductivity meter. Fig. 5(b) show that the order of the metals in corrosion rate and the effect of formic acid on corrosion resistance agreed with the results from immersion test in Fig. 4. In addition, the nyquist plot of zinc shows semicircle but the nyquist plots of iron

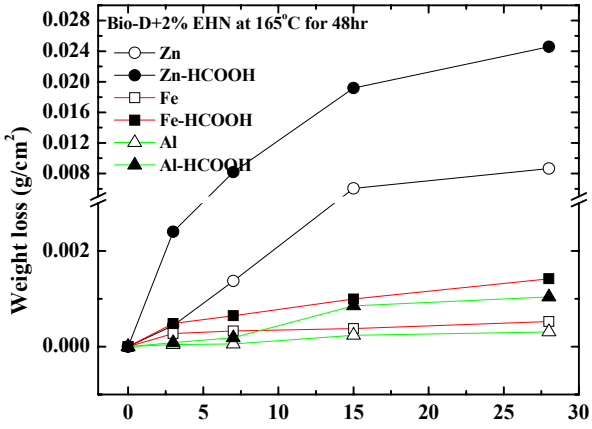

Fig. 4. Mass loss of metals with immersion in oxidized biodiesel.

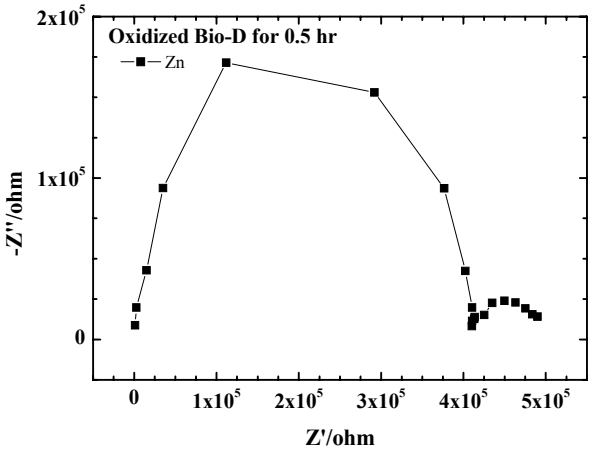

(a) Before subtraction of semi-circle

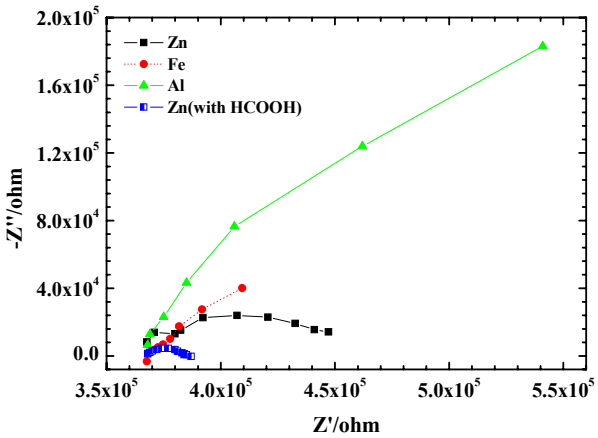

(b) After subtraction of semi-circle

Fig. 5. Nyquist plots of Zn, Fe, and Al in the oxidized biodiesel after 0.5-hour exposure: (a) Before subtraction of semi-circle, (b) After subtraction of semi-circle.

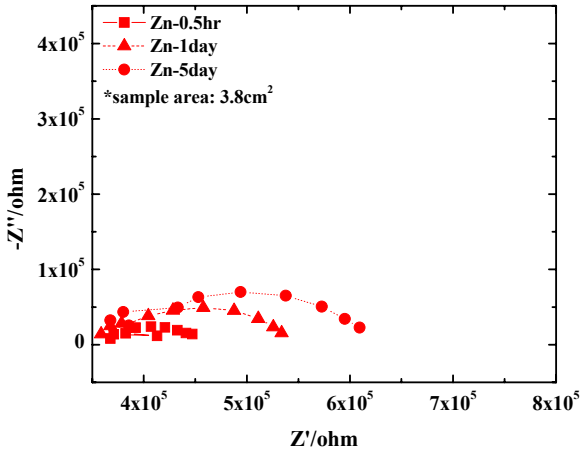

(a) Zn

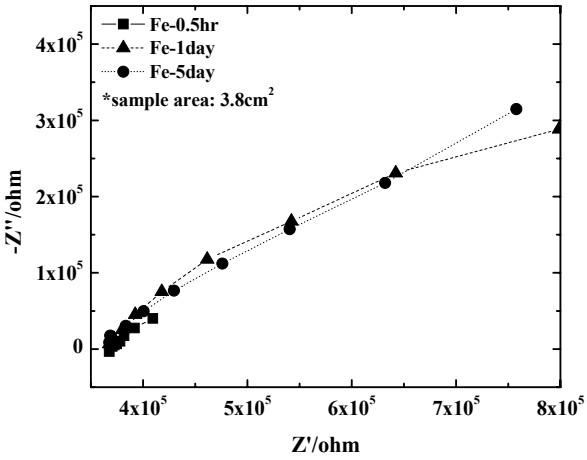

(b) Fe

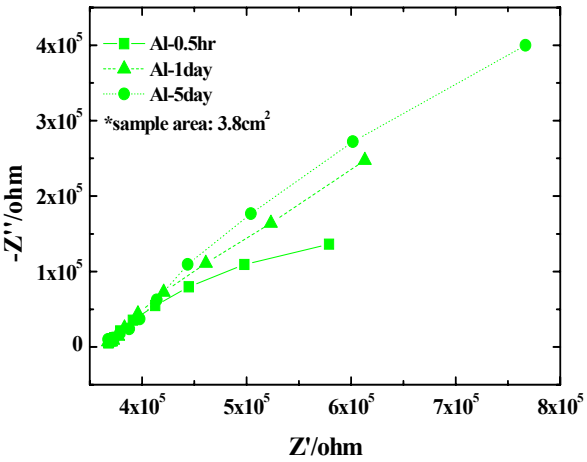

(c) Al

Fig. 6. Effect of immersion time on nyquist plots of (a) Zn, (b) Fe, and (c) Al in the oxidized biodiesel.

and aluminum does not. It means that corrosion of iron and aluminum are controlled by transfer through air-formed film or corrosion product film, while corrosion of iron is controlled by surface reaction, which agrees with the fact that the initial corrosion behavior of zinc conforms to linear behavior but the corrosion behaviors of iron and aluminum conform to parabolic behavior in Fig. 4. Furthermore, the nyquist plots of the metals in Fig. 6, shows that corrosion resistance increases with immersion time. Especially, the corrosion resistance of aluminum increased with immersion time as well as had the highest corrosion resistance.

3.2 Effects of Mg on corrosion resistance of Al-Mg alloys

Fig. 7 represents the effects of magnesium on anodic polarization curves of Al-Mg alloys in E55 and E85 con-

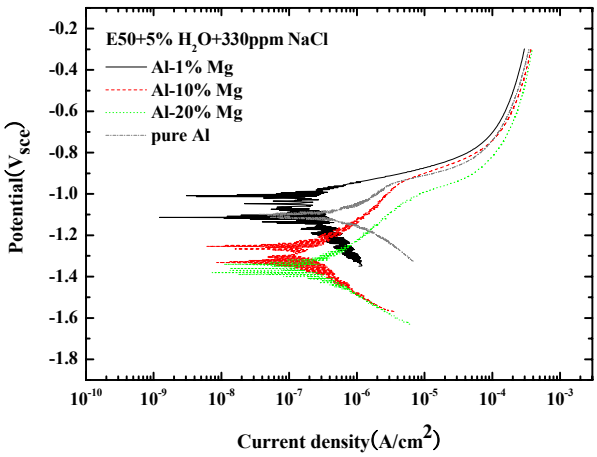

(a) E50*+330ppm NaCl

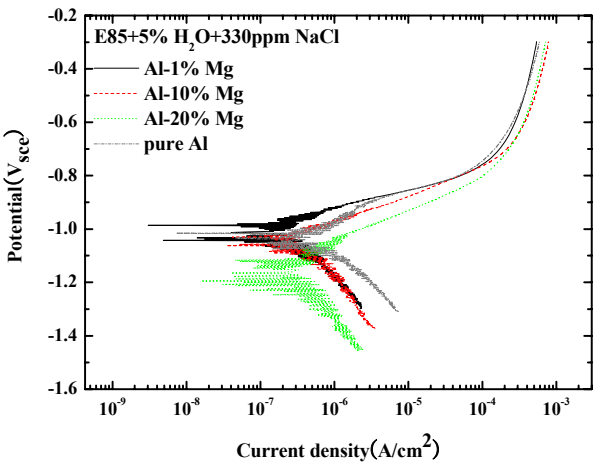

(b) E85*+330ppm NaCl

Fig. 7. Effect of Mg on polarization curves of Al-Mg alloys in (a) E50 containing 330ppm NaCl and (b) E85 containing 330 ppm NaCl.

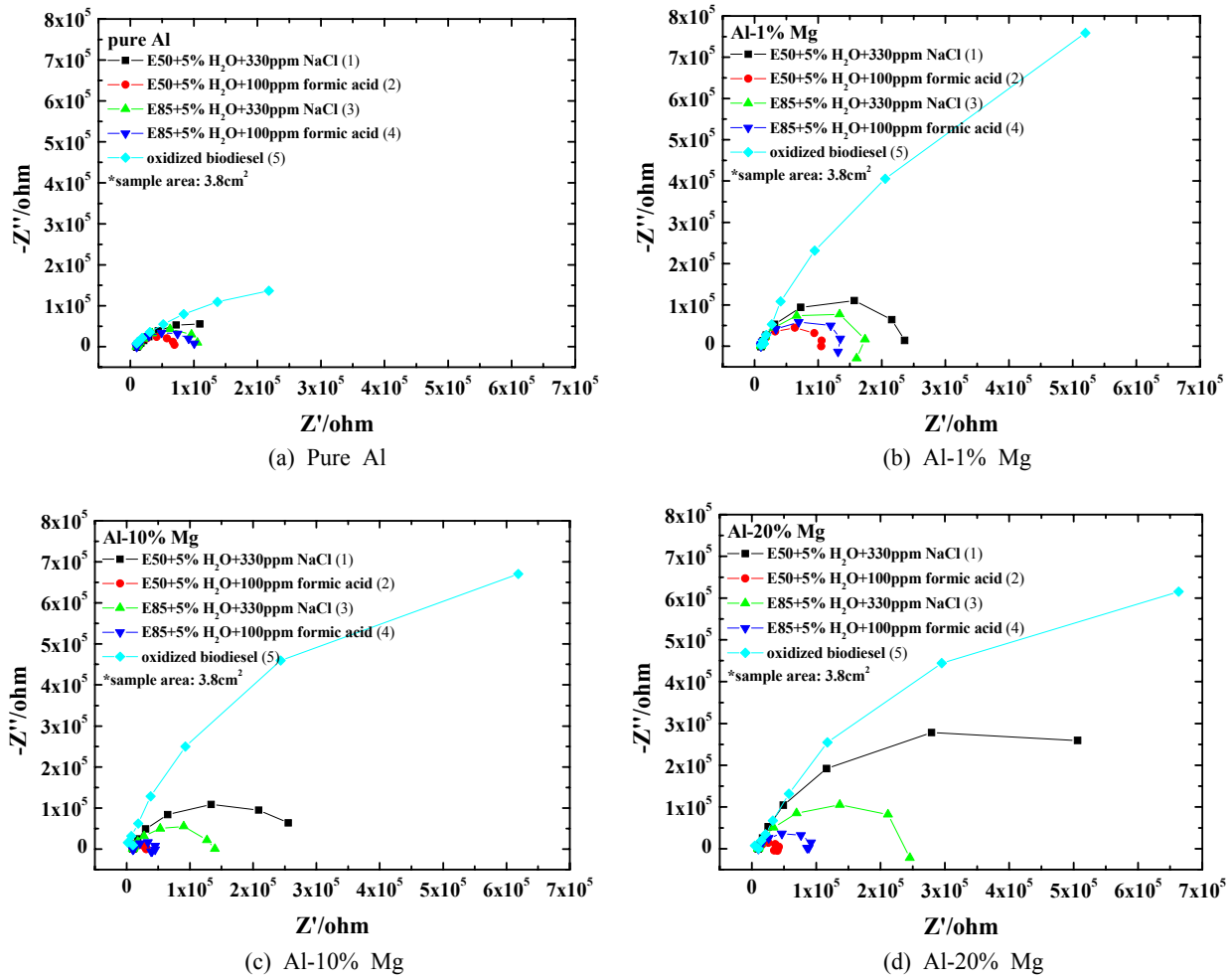

Fig. 8. Effect of Mg on nyquist plots of Al-Mg alloys in various gasoline/ethanol solutions and oxidized biodiesel: (a) pure Al, (b) Al -1% Mg, (c) Al -10% Mg, (d) Al -20% Mg.

taining NaCl. The addition of magnesium as an alloying element increased passive region about corrosion potential but decreased corrosion potential without the change of pitting potential. In addition, passive current was lowest in Al-1%Mg alloy but the further addition of magnesium increased the passive current density again. It indicates that magnesium effectively increase corrosion resistance around corrosion potential but can accelerate corrosion rate in oxidizing environments.

The noise issued from high resistance of solution makes it difficult to measure corrosion rate using Tafel extrapolation method. Furthermore, lower resistivity of gasoline/ethanol solution containing formic acid than NaCl (ρ of E50 with formic acid = 3.8 μS/cm, ρ of E50 with NaCl =80.1 μS/cm) has it impossible to conduct polarization test. To overcome the shortcoming of polarization test, twin two-electrode cells was used with EIS. The nyquist plots of Al-Mg alloys in various gasoline/ethanol solutions and the oxidized biodiesel are shown in Fig. 8, and the polarization resistances of Al-Mg alloys are summarized

Table 2. Polarization resistance (R_p) of Al-Mg alloys in gasoline/ethanol solutions and oxidized biodiesel calculated from nyquist plots in Fig. 8 and equivalent circuit in Fig. 3

Al alloys	Polarization resistance ($R_p(\Omega) \times 10^5$)				
	(1)*	(2)*	(3)*	(4)*	(5)*
Pure Al	1.780	0.616	0.976	0.929	7.045
Al-1%Mg	2.265	0.989	1.661	1.288	31.160
Al-10%Mg	2.805	0.220	1.296	0.368	16.690
Al-20%Mg	7.072	0.334	2.352	0.867	16.270

(1)*: E50+5% H_2O+330ppm NaCl,
(2)*: E50+5% H_2O+100ppm formic acid,
(3)*: E85+5%H_2O+330ppm NaCl,
(4)*: E85+5% H_2O+100ppm formic acid,
(5)*: oxidized biodiesel

in Table 2.

In gasoline/ethanol solutions containing NaCl, R_p from EIS increased with the addition of magnesium in Al-Mg alloys, which agrees with the results from polarization test that passive region is larger according to the addition of magnesium. In oxidized biodiesel, R_p's of Al-Mg alloys were much lower than those in the gasoline/ethanol solutions, and magnesium as an alloying element increased polarization resistance like gasoline/ethanol solutions containing NaCl. In gasoline/ethanol containing formic acid, the addition of magnesium did not increase R_p of Al alloy monotonously. In other words, Al-1% Mg had the highest R_p; however, Al-10% Mg and Al-20% Mg had lower R_p than pure Al. The decrease of polarization resistance of Al-10%Mg and Al-20% Mg is possibly related with the higher passive current density around potting potential as shown in Fig. 7. In other words, it can be due to the presence of an oxidizer such as formic acid as well as higher passive current density. Based on measurement of R_p of Al-Mg alloys, corrosivity increased in the order of oxidized biodiesel, gasoline/ethanol solution containing NaCl, and gasoline/ethanol solution containing formic acid.

4. Summaries

1) Combination of twin two-electrode cells and EIS make polarization resistances of metals (Zn, Fe, Al, and Al-Mg alloys) in solution with low resistivity measurable. It is proved by comparison between nyquist plots form EIS and anodic polarization curve or corrosion rate obtained from polarization test or immersion test, respectively.

2) From immersion test and EIS test, the corrosion resistance increased in the order of zinc, iron, and aluminum in oxidized biodiesel. The corrosion of iron and aluminum conforms to parabolic behavior while the corrosion of zinc conforms to linear behavior during only the initial immersion period.

3) Magnesium as an alloying element increased passive region but lowered corrosion potential without pitting potential. In addition, the passive current density of Al alloys increased with magnesium except Al-1%Mg.

4) In gasoline/ethanol solution containing NaCl and oxidized biodiesel, the addition of magnesium increased R_p effectively, while, in gasoline/ethanol solutions containing formic acid, the addition of more than 1% Mg degrades corrosion resistance. The corrosion resistance of Al-Mg alloys in gasoline/ethanol solutions containing formic acid can be explained with dependency of passive current density on magnesium added as an alloying element.

5) According to R_p's of Al-Mg alloys, corrosivity increased in the order of oxidized biodiesel, gasoline/ethanol solution containing NaCl, and gasoline/ethanol solution containing formic acid.

References

1. Frank Black, SAE TECHNICAL PAPER SERIES, 912413, SAE INTERNATIONAL, Toronto, Canada (1991).
2. Michael S. Graboski and Robert L. McCormick, *Prog. Energy Combust. Sci*., **24**, 125 (1998).
3. Alan C. Hansen, Qin Zhang, and Peter W.L. Lyne, *Bioresource Technology*, **96**, 277 (2005).
4. Lena SJogren, Magnus Nordling, and Jinshan Pan, CORROSION & METALS RESEARCH INSTIUTE, KIMAB-2007-103, 1 (2007).
5. Peter Hronsky, *National Association of Corrosion Engineers*, **37**, 161 (1981).
6. Heitz. E, Hukovic. M, and Maier, K.H., *Werkst. Korros*, **21**, 457 (1970).
7. R.D. Kane, J.G. Maldonado, and L.J. Klein, *NACE Int.*, **04543**, 1 (2004).
8. F. Bellucci, L. Nicodemo, and B. Licciardi, *Corros. Sci*., **27**, 1313 (1987).
9. A.M. Abdel-Gaber, H.H. Abdel-Rahman, A.M. Ahmed, and M.H. Fathala, *Anti-Corrosion Methods and Materials*, **53**, 218 (2006).
10. Sh. A. El-Shazly, A.A. Zaghloul, M.T. Mohamed, and R.M. Abdullah, *Anti-Corrosion Methods and Materials*, **42**, 9 (1995).
11. J. P. DE Souza, O. R. Mattos, L. Sathler, and H. Takenouti, *Corros. Sci*., **27**, 1351 (1987).
12. Howard L. Fang, Robert L. McCormick, SAE TECHNICAL PAPER SERIES, 2006-01-3300, SAE International, Toronto, Canada (2006).